E-Journal of Advanced Maintenance Vol.2 (2010/2011) 181-190
Japan Society of Maintenology

Efficient Transduction of Circumferential Lamb Waves by a Pair of Line Focus Type Noncontact Air-coupled Ultrasonic Transducers and its Application for Accurate Measurement of Pipe Wall Thickness

Hideo NISHINO[1,*], Kenichi YOSHIDA[1], Tadashi ASANO[1], Yuta TANIGUCHI[1], Hitoshi OGAWA[2], Masakazu TAKAHASHI[3], Yukio OGURA[3]

[1] *The University of Tokushima, 2-1 Minami-josanjima, Tokushima-city, Tokushima 770-8506, Japan*
[2] *Tokushima Prefectural Industrial Technology Center, 11-2 Saikai, Saiga-town, Tokushima-city, Tokushima 770-8021, Japan*
[3] *Japan Probe Co. Ltd., 1-1-14 Nakamura-town, Minami-ward, Yokohama-city, Kanagawa 232-0033, Japan*

ABSTRACT

Efficient transduction of a circumferential (C-) Lamb wave by a pair of noncontact air-coupled ultrasonic transducers (NAUTs) was presented. A line focus type (LFT-) of the NAUT was employed for the efficient transduction of the C-Lamb wave, which was designed so as to take an almost same angle of the incident longitudinal beam on the circular pipe surface. Outstanding characteristics of the LFT-NAUT for the C-Lamb wave transduction were theoretically and experimentally shown in comparison to those of the conventional plane type (CPT-) NAUT. The efficiency of the C-Lamb wave generated and detected by the LFT-NAUT took about 20 times higher than that by the CPT-NAUT. As for an application of the C-Lamb wave generated by the LFT-NAUT, a novel method of an accurate estimation of pipe wall thickness was introduced and evaluated with a theoretical model. It was confirmed that the maximum error between the experiments and the theoretical model was at around 10 μm.

KEYWORDS

ultrasonic, nondestructive evaluation, pipe wall thinning, Lamb wave, circumferential Lamb wave, guided wave, health monitoring, noncontact air-coupled ultrasonic transducer

ARTICLE INFORMATION

Article history:
Received 22 November 2010
Accepted 3 February 2011

1. Introduction

Noncontact air-coupled ultrasonic transducer (NAUT) is one of the powerful tools for monitoring the condition of various materials because of its noncontacting nature. Recently, highly sensitive NAUT [1-3] consisted of piezoelectric pillars embedded in a polymer matrix (so-called composite transducer) have been exploited with their optimized electronics. Because of the condition for the transverse resonance [4] of a plate specimen, effective transduction of the Lamb waves rather than the bulk acoustic waves is easily realized [3] by the NAUT. Thus, the noncontact generation of the Lamb wave by the NAUT is a useful tool to evaluate plate specimens because of its noncontacting nature. Therefore, many applications for plate specimens using the NAUT have been presented. Measurements of anisotropy [5], thickness [6-9] and adhesive quality [10] of plates have been proposed and carried out using the NAUT.

A circumferential (C-) Lamb wave [11-18] propagating along the circumference of the pipe has also been generated [19] by the NAUT for a wall thickness measurement of piping. In general, an efficient transduction of the Lamb or the C-Lamb wave can be achieved in accordance with the critical angle incidence of the longitudinal wave from the air to the surface of the solid specimen. The efficient condition [3] of the critical angle incidence is easily achieved for the Lamb wave transduction; however, it is very difficult for the C-Lamb wave transduction to meet the efficient condition because of the curved surface of the pipe. Namely, the incident angle of the plane wave to the circular surface of the pipe varies depending on the position of the incidence. To solve this problem, this paper proposes a novel and efficient transduction method for the C-Lamb wave using line focus type (LFT-) NAUTs. The method can maintain almost constant incident angle to the

*Corresponding author, Tel: 81-88-656-7357, Fax: 81-88-656-9062, E-mail: nishino@me.tokushima-u.ac.jp

circular surface so as to generate and detect the C-Lamb wave effectively. The principle and characteristics of the method were presented in this paper.

On the other hand, the authors proposed and evaluated [19, 20] an accurate measurement of a pipe wall thickness using the C-Lamb wave generated by the conventional plane type (CPT-) NAUT having a flat aperture. The principle of the measurement is fundamentally based on the precise detection of an angular wave number of the C-Lamb wave depending on the wall thickness of the pipe. In this paper, measurements of the wall thicknesses were carried out with a pair of the LFT-NAUTs according to the principle. After describing briefly the principle of the accurate estimation of the pipe wall thickness, the experimental verifications were shown. The experimental estimations of the wall thicknesses agreed excellently with both the actual thicknesses measured by the thickness-meter and the calculation results of the mathematical model based on the theory described. It was confirmed that the maximum error of the experiments to theoretical calculations was around 10 μm.

2. Characteristics of line focus type NAUT for C-Lamb wave transduction

In this section, important characteristics for the generation of the C-Lamb wave using the critical angle incidence of the longitudinal wave in the air to a circular surface using the LFT- and CPT-NAUT were presented.

The relationship between the pipe specimen (outer radius: R) and the flat aperture of the CPT-NAUT is shown in Fig. 1(a). It is very easy to understand that the incident angle i of the longitudinal wave from the flat aperture to the pipe surface is completely equal to the angular position φ of the pipe.

On the other hand, the relationship between the pipe specimen and the concave aperture of the LFT-NAUT (focal length: R_F) is shown in Fig. 1(b). The angular position of the pipe is also described as a function of φ. The focal point of the LFT-NAUT assumes to be at x_1 on the x-axis. The angle of a beam tracing of the longitudinal wave from the centerline of the LFT-NAUT is describe as a function of θ as depicted in Fig. 1(b). The incident angle i to the pipe surface and the phase velocity v_p on the pipe surface with respect to the LFT-NAUT are shown in Eqs. (1) and (2), respectively.

$$i = \tan^{-1}\left(\frac{x_1 \cos\varphi}{R - x_1 \sin\varphi}\right), \tag{1}$$

$$v_p = \frac{v_{air}}{\sin i}, \tag{2}$$

where v_{air} is the longitudinal velocity of the air. The propagation distance d_{CPT} of the longitudinal wave between the pipe surface and the flat aperture and the propagation distance d_{LFT} between the pipe surface and the concave aperture, respectively, are

$$d_{CPT} = D - R\cos\varphi, \tag{3}$$

$$d_{LFT} = R_F - \sqrt{R^2 + x_1^2 - 2Rx_1 \sin\varphi}, \tag{4}$$

where D is the distance between the flat aperture and the x-axis, as shown in Fig. 1(a). Since the phase advance of the longitudinal wave propagation from the aperture to the pipe surface is as same as the phase on the pipe surface. Thus the phases p_{CPT} and p_{LFT} on the pipe surface are

$$p_{CPT} = k_{air} d_{CPT}, \tag{5}$$

$$p_{LFT} = k_{air} d_{LFT}, \tag{6}$$

where k_{air} is the wave number of the longitudinal wave in the air. The phase on the pipe surface as well as the incident angle is one of the most important parameters to generate the C-Lamb wave effectively. That is, the C-Lamb waves are effectively generated when the phase on the pipe surface equals those of the C-Lamb waves.

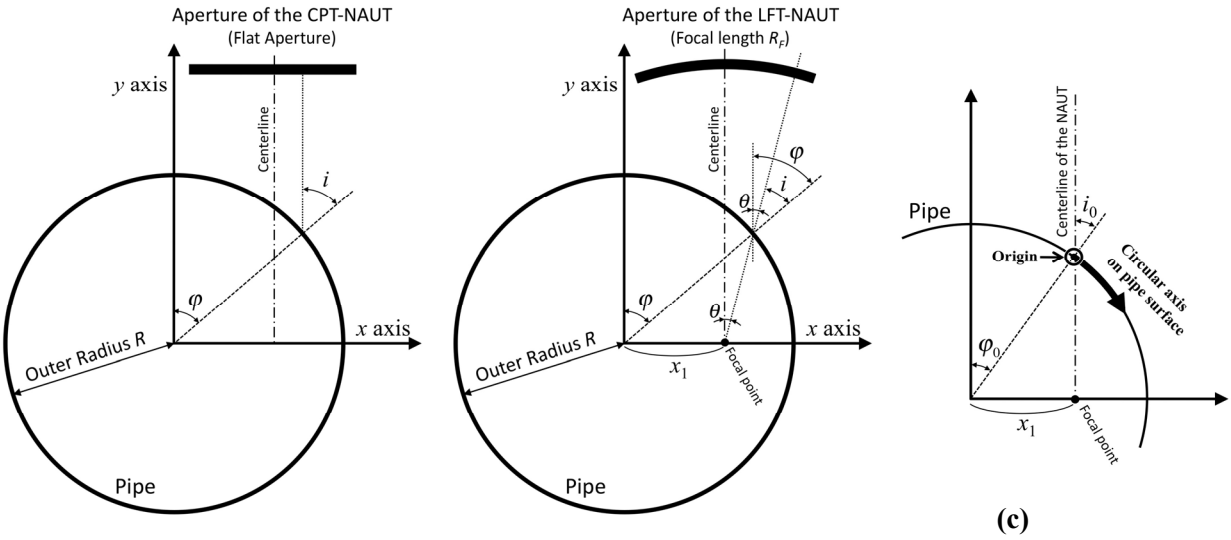

(a) **(b)** **(c)**

Fig. 1. Coordinate systems and variables used in the calculations for the CPT-NAUT (a), the LFT-NAUT (b) and the circular axis on the pipe surface (c).

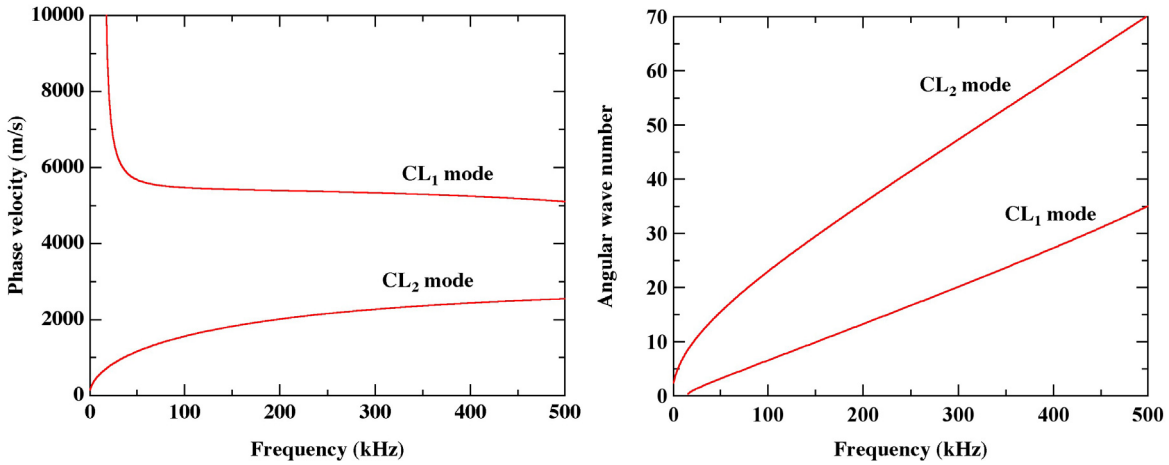

(a) **(b)**

Fig. 2. Dispersion relations of the phase velocity (a) and angular wave number (b) of the 114.1 mm outer diameter and 3 mm thick aluminum pipe.

In the following experimental verifications, we focused on the transduction in the CL_2 mode of the C-Lamb wave at the frequency range around 310 kHz propagating along the 114.1 mm outer diameter and 3 mm thick aluminum (Al) pipe. Figures 2(a) and 2(b) show the dispersion relations of the phase velocity and angular wave number of the Al pipe, respectively. The CL_1 and CL_2 modes are very similar to the A_0 and S_0 modes of the Lamb wave generated in a plate specimen, respectively. Figure 3 shows the incident angle regarding to both the CPT- and LFT-NAUT as a function of the location on the circular axis along the outer circumference of the pipe (see Fig. 1(c)). The origin of the circular axis set at the intersection of the pipe surface and the centerline of the each transducer, as shown in Fig. 1(c). That is, the origin of the circular axis is where the angular position φ takes φ_0 as shown in Fig. 1(c). The parameters used in the calculations are summarized in Table 1. Since the x_1 set to be 8.47 mm, the incident angle and the phase velocity at the origin of the circular axis are 8.53˚ and 2290 m/s, respectively. This value of the phase velocity equals the phase velocity of the CL_2 mode of the C-Lamb wave at 310 kHz, as shown in Fig. 2. As shown in Fig. 3, the incident angle for the LFT-NAUT takes an almost same value at around 8.53˚ (from 8.22˚ to 8.53˚ in the range of ±15 mm) while the incident angle for the CPT-NAUT is almost linearly and considerably changed as a function of the location on the circular axis. In the Lamb and C-Lamb waves generation by the critical angle method, an accuracy of the angle of incidence is of extremely importance especially in the air-coupled transductions [3].

Table 1 Parameters used in the calculations

Outer radius of pipe R (mm)	Focal length R_F (mm)	Focal point on x-axis x_1 (mm)	Velocity of the air v_{air} (m/s)
57.1	110	8.47	340

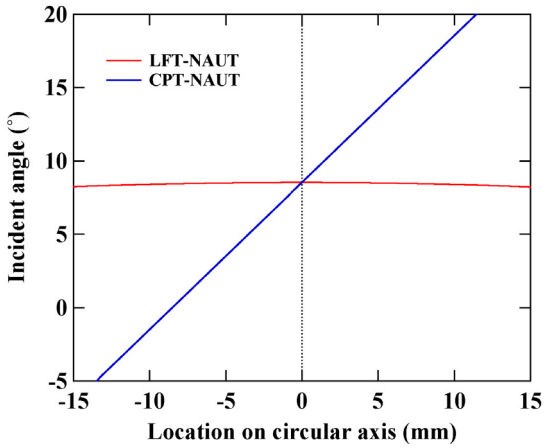

Fig. 3. Incident angle as a function of the location on the circular axis. The incident angle of the LFT-NAUT is almost constant in the range of ±15 mm.

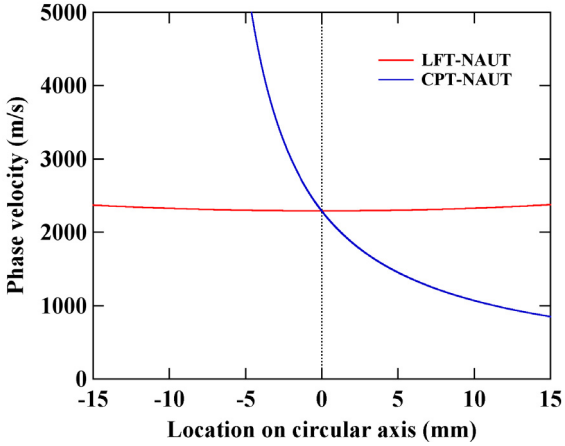

Fig. 4. Phase velocity as a function of the location on the circular axis. The phase velocity of the LFT-NAUT is almost constant in the range of ±15 mm.

The phase velocity on the pipe surface calculated by eq. (2) is shown in Fig. 4. As for the CPT-NAUT, the phase velocity is drastically changed as a function of the location on the pipe surface. In contrast to the case of the CPT-NAUT, the phase velocity in the LFT-NAUT is also takes an almost constant value around 2290 m/s (from 2290 to 2370 m/s in the range of ±15 mm).

Spatial distributions of the phases on the circular axis for the CPT- and LFT-NAUT are shown in Figs. 5(a) and 5(b), respectively, while the phase on the apertures equals 0˚. As for the LFT-NAUT depicted in Fig. 5(b), the spatial distribution is almost linearly distributed and equal to that of the CL_2 mode C-Lamb wave at the frequency of 310 kHz in the range of ±15 mm on the circular axis. In contrast to this, as for the CPT-AUT, the spatial distribution varies nonlinearly and equals that of the CL_2 mode C-Lamb wave only at around the origin of the circular axis.

As shown in the above explanations for the LFT- and CPT-NAUT, the characteristics of the LFT-NAUT are quite optimized for the transduction of the C-Lamb waves. The following chapter shows the experimental verifications of the LFT-NAUT for the C-Lamb wave transduction and its application.

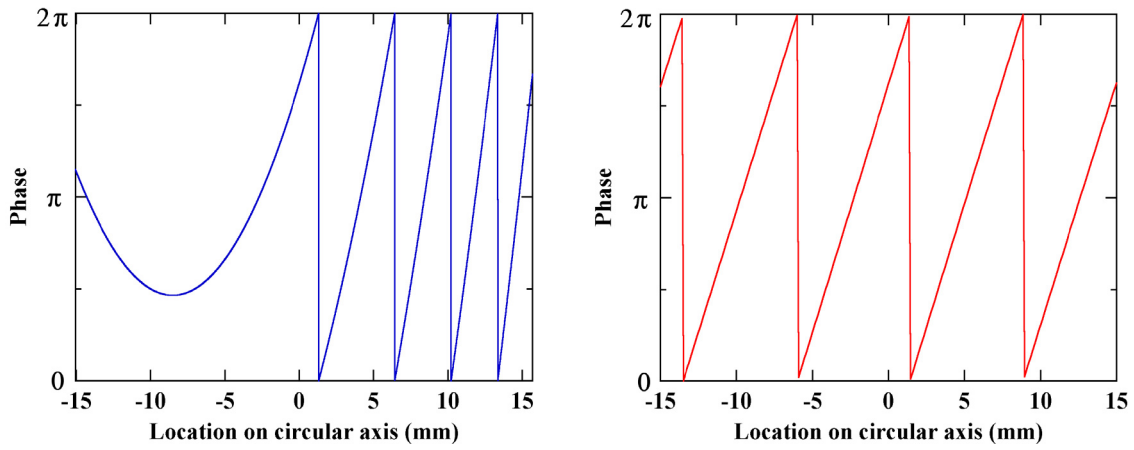

Fig. 5. Spatial phase distributions on the circular axis for the CPT-NAUT (a) and the LFT-NAUT (b). The spatial phase distribution generated by the LFT-NAUT is almost linearly allocated on the circular axis and is as almost same as that of the CL_2 mode of the C-Lamb wave.

3. Experimental verification

3.1. Experimental apparatus

An illustration of the experimental setup is depicted in Fig. 6. A face-to-face setting of a pair of the LFT-NAUTs as the transmitter and receiver, respectively, was used for the transduction of the C-Lamb waves. The two transducers were located at their confocal positions. A pair of the CPT-NAUT was also used for comparison. The aperture sizes of both the LFT-NAUT and the CPT-NAUT are 20 x 60 mm^2 and 14 x 20 mm^2, respectively. The center frequencies of the LFT-NAUT and the CPT-NAUT are 310 and 340 kHz, respectively, which are depending on the electric capacitances of both transducers mainly related to their aperture sizes. Namely, the aperture area of the LFT-NAUT is 4.3 times larger than that of the CPT-NAUT. 10- and 130-cycle tone-burst signals were generated (Tektronix AFG3102) and amplified (NF BA4825) to 20 V peak-to-peak for the LFT-NAUT and to 200 V for the CPT-NAUT and fed into the transmitters to generate the CL_2 mode C-Lamb waves. The difference of the input voltages between the two transducers is depending on the sensitivities for the transduction of the C-Lamb wave between them. The received signals for the both transducers were amplified (NF 9311 and NF3628) 90 dB. A digital oscilloscope (Tektronix DPO7054) was employed to observe and store the signals detected. 300 times averaging sequence in the digital oscilloscope and the 10 kHz width 48dB/Oct band-pass filter were used to improve the signal to noise ratio (S/N). 114.1 mm outer diameter and 3 mm thick Al pipes were used. 10 different wall thinnings (up to around 1.0 mm) were introduced to the inner surface of the Al pipes by a lathe. A universal length-measuring machine (Tsugami T-ULM500) having 1 μm nominal accuracy was used to measure the wall thicknesses of all the Al pipes. Table 2 shows the averaged wall thickness losses of all the specimens used in the experiments. The details of the specimens were described in ref. [20].

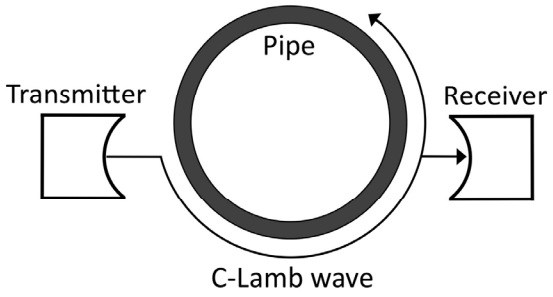

Fig. 6. Schematic illustration of the experimental apparatus of the two NAUTs, the Al pipe specimen and the C-Lamb wave circling along the pipe

Table 2 Wall thickness losses and their standard deviations

Sample No.	1	2	3	4	5	6	7	8	9	10
Loss of wall (mm)	0.000	0.098	0.254	0.398	0.439	0.544	0.641	0.764	0.876	1.016
Std. dev. (mm)	0.025	0.019	0.032	0.020	0.029	0.032	0.027	0.053	0.025	0.035

To generate and detect the CL_2 mode of the C-Lamb wave effectively, the procedure for setting the pair of the transducers to the pipe specimen was introduced as follows:

(1) Locate the pair of the LFT-NAUTs at a confocal face-to-face position so as to take the maximum amplitude without the pipe specimen. As for the pair of the CPT-NAUTs, achieve only the face-to-face location.
(2) Insert the pipe specimen between the pair of the transducers.
(3) Search the optimum location of the pipe specimen for the effective transduction so as to take the maximum amplitude of the CL_2 mode of the C-Lamb wave generated. It can be obtained while the angle of incidence takes precisely the critical angle for the transductions.

3.2. Verification for the transduction efficiency

Time domain signals of the CL_2 mode of the C-Lamb wave generated and detected by the pairs of both the CPT-NAUTs and the LFT-NAUTs are shown in Figs. 7(a) and 7(b), respectively. The 10-cycle toneburst signals were used for the generations in the both cases. The center frequencies of the toneburst signals were 340 kHz for the CPT-NAUT and 310 kHz for the LFT-NAUT, which were as same as the center frequencies of the transducers, respectively. The three wave packets could be seen in the both cases. The first wave packet (0th lap wave) was the wave that was generated by the transmitter, and was detected by the receiver after propagating roughly half along the circumference of the pipe (see Fig. 6). The second and third wave packets (1st and 2nd lap waves) in Figs. 7(a) and 7(b) were the waves that have propagated roughly 1.5 and 2.5 turns along the circumference of the pipe, respectively.

The amplitudes of the first wave packets generated and detected by the CPT- and LFT-NAUT were 0.37 and 0.75 V peak-to-peak, respectively. Therefore, the multiplication of the transduction efficiency of both the transmission and reception of the CL_2 mode for the LFT-NAUT was almost 20 times larger than that for the CPT-NAUT because the amplitude of the input signals for the CPT-NAUT is 10 times larger than that for the LFT-NAUT as described in the previous section. On the other hand, the aperture area of the LFT-NAUT is 4.3 times larger than that of the CPT-NAUT, this means that the efficiency per a unit aperture-area of the LFT-NAUT is 4.3 times larger than that of the other transducer. Anyway, not the CPT-NAUT but the LFT-NAUT has taken the ability to maintain the optimized angle of incidence on wider surface of the pipe for much efficient transduction. Therefore, it can be estimated that the transduction efficiency of the CPT-NAUT won't be increased with an increase of the aperture area; conversely, that of the LFT-NAUT will be increased with it. It was clearly confirmed that the transduction efficiency of the CL_2 mode of the C-Lamb wave for the LFT-NAUT was much higher than that for the CPT-NAUT at the respective center frequencies.

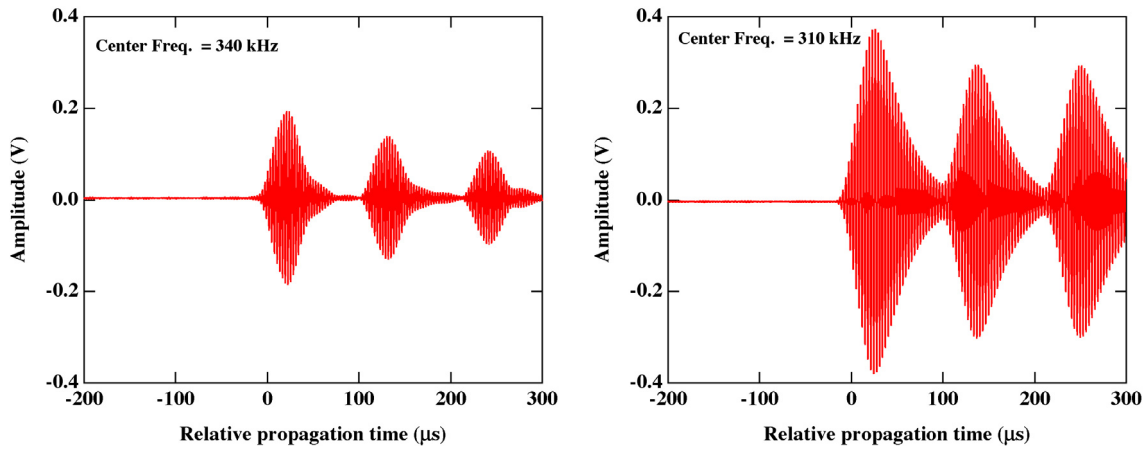

Fig. 7. Typical time domain signals generated and detected by the CPT-NAUT (a) and the LFT-NAUT (b).

3.3. Experimental estimation of the pipe wall thinning using a pair of LFT-NAUTs

An accurate estimation method [19, 20] of a pipe wall thickness by detecting a minute difference of an angular wave number of the C-Lamb wave is briefly described. Figure 8 shows the angular wave number as a function of the frequency for four different wall thinnings at around the center frequency 310 kHz of the LFT-NAUT. The angular wave number is the least increased with an increase of the wall thickness loss. Thus, it is too difficult to detect such a small difference of the angular wave number using a conventional time-of-flight method. On one hand, in the present method, the generation and detection of the C-Lamb wave was realized in the same manner described in the section 3.1. That is to say, the C-Lamb wave circling along the circumference of the pipe was efficiently transmitted and received by a pair of the LFT-NAUT. On the other hand, for the accurate detection of the angular wave number, a tone burst signal having a large number of cycles (130-cycles) is used so as to superpose the C-Lamb wave itself on its own propagation orbit. In this setting, the amplitude of the superposed regions changes considerably owing to the change of the wave number of the C-Lamb wave. The amplitude A of the superposed region is

$$A = \left| \sum_{m=0}^{n} A_n \exp\left(2\pi \mathrm{i} mp\right) \right|, \tag{7}$$

where n, A_n and p are number of the superposition, amplitude of each circling wave and angular wave number of the C-Lamb wave, respectively. Figure 9 shows calculated amplitudes (n=1) for various wall thinnings as a function of frequency. The amplitude peaks shifted on the frequency axis with an increase of wall thinning.

The typical time domain signals of the CL_2 mode of the C-Lamb waves propagating in the pipe without any wall thickness loss are shown in Fig. 10, which were generated by 130 cycle tone burst signals. In contrast to the time domain signals generated by 10-cycle tone burst signals (Fig. 8), it was confirmed that all the wave packets were extremely long and were superposed onto themselves. Therefore, it was clearly confirmed that the amplitude of the superposed region (after 100 μs) was drastically changed owing to the frequency as shown in Fig. 10. This phenomenon was the result of the relative phase differences between the 0th, 1st and 2nd lap waves owing to the change of the frequency. The normalized amplitude as a function of frequency for the wall thickness losses of 0.000, 0.098, 0.254 and 0.398 mm is shown in Fig. 11. The amplitude at the mid time of the each superposed region was measured. The mid times of the 1st and 2nd superposed regions were 180 and 300 μs, which were determined by eye using the time domain signals of 310 kHz (the center frequency of the LFT-NAUT) as shown in Fig. 10. In comparison to the theoretical results shown in Fig. 9, it could be found that the peak amplitudes changed with a change of the frequency because of the center frequency (310 kHz) of the LFT-NAUT as shown in Fig. 11. In contrast to this, the peak frequencies were almost same as those estimated by the theoretical calculations as shown in Fig. 9. The peak frequency in Fig. 11 as a function of wall thickness loss is summarized in Fig.12. Red circles and blue dotted lines are the experimental results and the theoretical calculations, respectively. To determine the experimental peak frequency of the characteristic-curve in Fig. 11, a least square fitting to the Gaussian-curve was applied to each region around the peak. The theoretical calculations (the blue doted lines in Fig. 12) were carried out on the basis of ref. [13] with the longitudinal and transverse wave velocities (v_l = 6400 m/s, v_t = 3040 m/s) of Al material. It was obviously confirmed that the experimental results agreed excellently with the theoretical calculations. The maximum error between the experiments and theory was around 10 μm, which was as almost same as that obtained by the CPT-NAUT [19, 20]. This result means that the accuracy of the method for the wall thickness estimation is not improved although the transduction efficiency of the LFT-NAUT is increased extremely. On the other hand, the robustness of the method using the LFT-NAUT must be increased so much in actual noisy situations because of its efficient sensitivity.

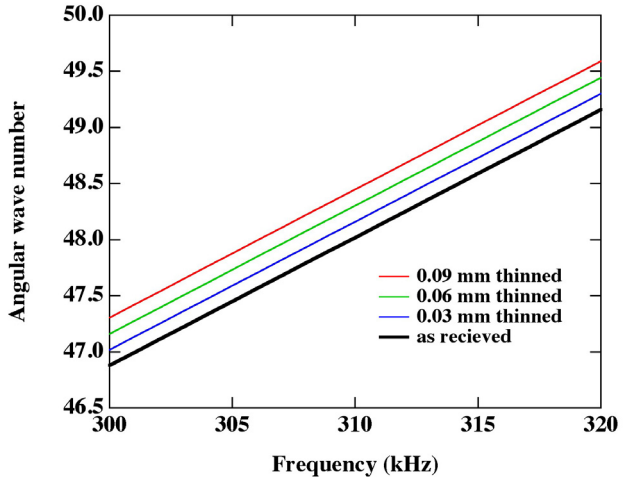

Fig. 8. Dispersion relation of the angular wave number of the C-Lamb wave for different wall thinnings at around the center frequency of the LFT-NAUT.

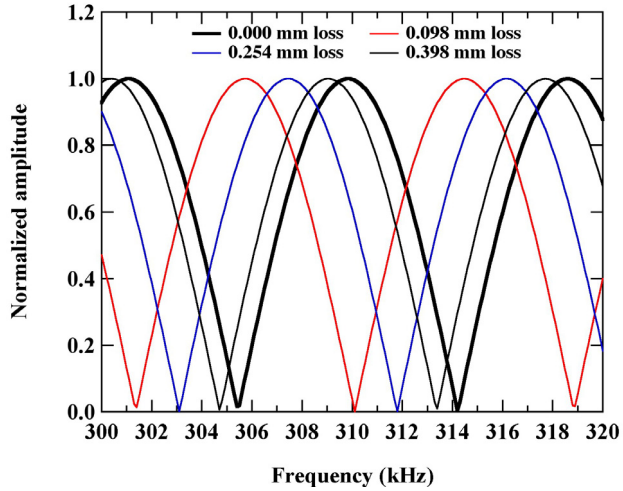

Fig. 9. Calculated normalized amplitude of the superposed region (0th and 1st laps) as a function of the frequency

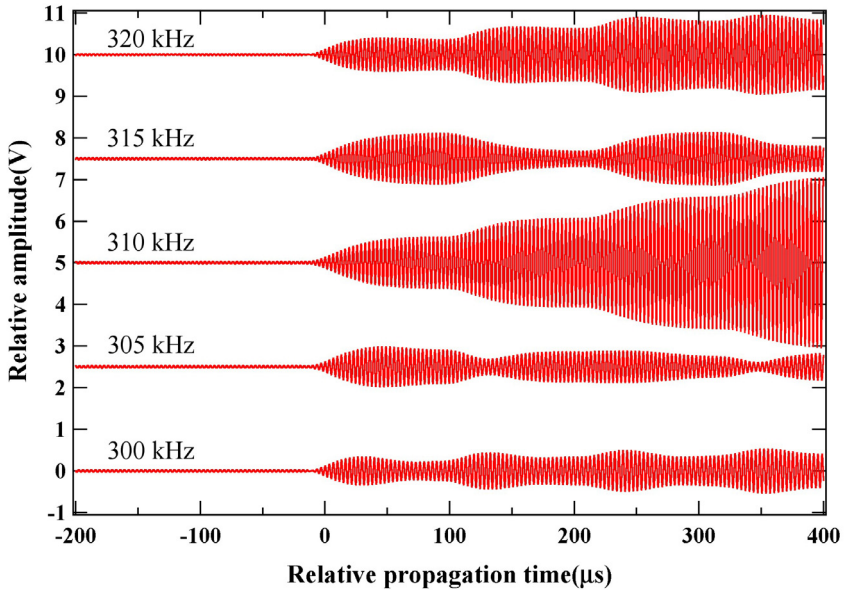

Fig. 10. Time domain signals of the CL_2 mode generated by 130-cycle tone bursts for different center frequencies. The amplitude of the superposed regions changed owing to the frequency.

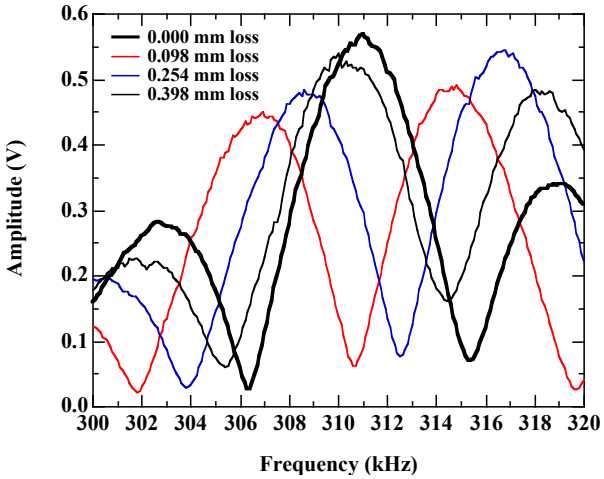

Fig. 11. Amplitude of the superposed region (0th and 1st laps) as a function of the frequency

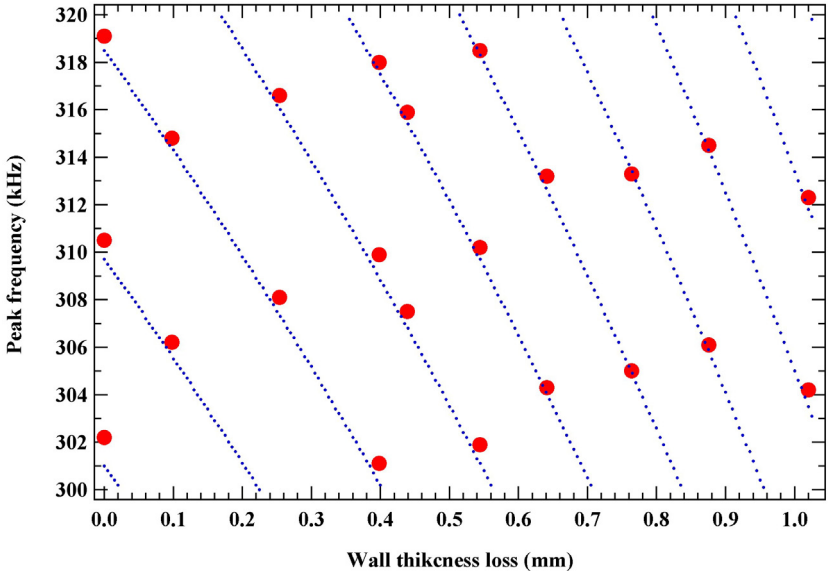

Fig. 12. Peak frequency as a function of wall thickness loss. Red circles and blue dotted lines indicate experimental results and theoretical estimation.

4. Conclusion

This paper describes a novel and extremely efficient method for the transduction of the circumferential (C-) Lamb wave using a pair of the line focus type (LFT-) noncontact air-coupled ultrasonic transducers (NAUTs) and its application for a wall thickness measurement of a pipe. Comparing to the conventional plane type (CPT-) NAUT, the outstanding characteristics of the LFT-NAUT for the highly efficient transductions were presented as follows:

(1) The incident angle of the longitudinal wave in the air to the circular pipe surface is almost constant as a function of the circular position.
(2) Corresponding to the constant angle of the incidence, the phase velocity on the circular surface of the pipe is also almost constant for the efficient transduction.
(3) The spatial distribution of the phase on the circular surface emerged by the incidence of the longitudinal wave in the air is also almost constant for the efficient transduction.
(4) In the experimental verifications, the transduction efficiency of the LFT-NAUT was 20-times larger than that of the CPT-NAUT. The highly efficient transduction was clearly confirmed.

As for the verification of wall thickness measurements using the LFT-NAUT, the accuracy of the results was around 10 μm. The highly accurate estimation of the wall thickness together with the extremely high transduction efficiency has been achieved in noncontact manner using the LFT-NAUT.

Acknowledgement

This work was partially supported by an academic grant from the Condition Monitoring Technology (CMT) division of the Japan Society of Maintenology (JSM).

References

[1] R. Farlow and G. Hayward, Real-time ultrasonic techniques suitable for implementing noncontact NDr systems employing piezoceramic composite transducers, Insight 36 (1994), 926-935.
[2] M.Castaings and P. Cawley, The generation, propagation, and detection of Lamb waves in plates using air-coupled ultrasonic transducers, Journal of the Acoustical Society of America 100 (1996), 3070 -3077.
[3] H. Nishino, S. Masuda, K. Yoshida, M. Takahashi, H. Hoshino, Y. Ogura, H. Kitagawa, J. Kusumoto and A. Kanaya, Theoretical and Experimental Investigations of Transmission Coefficients of Longitudinal Waves through Metal Plates Immersed in Air for Uses of Air Coupled Ultrasounds, Materials Transactions 49 (2008), 2861-2867.
[4] B. A. Auld, *Acoustic fields and waves in solids II Second Edition*, Krieger Publishing Co., 1990, p76.
[5] I. Yu. Solodov, R. Stoessel and G. Busse, Material Characterization and NDE Using Focused Slanted Transmission Mode of Air-Coupled Ultrasound, Research in Nondestructive Evaluation 15 (2004), 65-85.
[6] D. Tuzzeo and F. Lanza di Scalea, Noncontact Air-Coupled Guided Wave Ultrasonics for Detection of Thinning Defects in Aluminum Plates, Research in Nondestructive Evaluation 13 (2001), 61-77.
[7] M. Watanabe, M. Nishihira and K. Imano, Detection of Defects on Reverse Side of Metal Plate Using MHz-Range Air-Coupled Lamb Wave, Japanese Journal of Applied Physics 45 (2006), 4565-4568.
[8] M. Castainings, P. Cawley, R. Farlow and G. Hayward, Single Sided Inspection of Composite Materials Using Air Coupled Ultrasound, Journal of Nondestructive Evaluation 17 (1998), 37-45.
[9] S. H. Holland and D. E. Chmenti, Air-coupled acoustic imaging with zero-group-velocity Lamb modes, Applied Physics Letters 83 (2003), 2704-2706.
[10] D. W. Schindel, D.S. Forsyth, D.A. Hutchins and A. Fahr, Air-coupled ultrasonic NDE of bonded aluminum lap joints, Ultrasonics 35 (1997), 1-6.
[11] X. Zhao and J. L. Rose, Guided circumferential shear horizontal waves in an isotropic hollow cylinder, Journal of the Acoustical Society of America 115 (2004), 1912-1916.
[12] H. Nishino and K. Yoshida, Simple method of generating for circumferential shear horizontal waves in a pipe and their mode identifications, Acoustical Science and Technology 27 (2006), 389-392.
[13] H. Nishino, R. Yokoyama, H. Kondo and K. Yoshida, Generation of Circumferential Guided Waves Using a Bulk Shear Wave Sensor and their Mode Identification, Japanese Journal of Applied Physics 46 (2007), 4568 -4576.
[14] H. Nishino, R. Yokoyama, K. Ogura, H. Kondo and K. Yoshida, Tone-Burst Generation of Circumferential Guided Waves by a Bulk Shear Wave Sensor and Their Wide-Range Time–Frequency Analyses, Japanese Journal of Applied Physics 47 (2008), 3885-3893.
[15] M. Hirao and H. Ogi, An SH-wave EMAT technique for gas pipeline inspection, NDT & E International 32 (1999), 127-132.
[16] S. Li, T. Okada and X. Chen, Electromagnetic Acoustic Transducer for Generation and Detection of Guided Waves, Japanese Journal of Applied Physics 45 (2006), 4541-4546.
[17] H. Nagamizo, K. Kawashima and J. Miyauchi, NDE of pipe inner corrosion with delayed echoes of SV wave propagated circumferentially in liquid –filled pipes, Proc. Pressure Vessel and Piping 2003, p.7-12.
[18] W. Luo, J. L. Rose, J. K. Van Velsor, M. Avioli and J. Spanner, Circumferential guided waves for defect detection in coated pipe, Rev. of Progress in QNDE 820 (2005), 165-172.
[19] H. Nishino, T. Asano, K. Yoshida, H. Ogawa, M. Takahashi and Y. Ogura, Noncontact and Accurate Measurement of Pipe Wall Thinning by a Circumferential Lamb Wave Using a Pair of Air-Coupled Transducers, Proc. of 23rd International Congress on Condition Monitoring and Diagnosis Engineering Management, Eds. S. Okuma et al, June 2010, Nara Japan, pp.163-168.
[20] H. Nishino, Y. Taniguchi, T. Asano, K. Yoshida, H. Ogawa, M. Takahashi and Y. Ogura, Precise measurement of pipe wall thickness in noncontact manner by a circumferential Lamb wave generated and detected by a pair of air-coupled transducers, to be published in Japanese Journal of Applied Physics 50 (2011).